

Relationship Between Dynamic Tensile Strength and Pore Structure of Saturated Concrete under Lateral Pressure

Wang, Hao; Wang, Licheng; Ghiassi, Bahman; Song, Yupu; Zhou, Le; Hou, Dongxu

DOI:

[10.1007/s12205-022-0567-6](https://doi.org/10.1007/s12205-022-0567-6)

License:

Other (please specify with Rights Statement)

Document Version

Peer reviewed version

Citation for published version (Harvard):

Wang, H, Wang, L, Ghiassi, B, Song, Y, Zhou, L & Hou, D 2023, 'Relationship Between Dynamic Tensile Strength and Pore Structure of Saturated Concrete under Lateral Pressure', *KSCCE Journal of Civil Engineering*, vol. 27, no. 3, pp. 1166–1173. <https://doi.org/10.1007/s12205-022-0567-6>

[Link to publication on Research at Birmingham portal](#)

Publisher Rights Statement:

This version of the article has been accepted for publication, after peer review (when applicable) and is subject to Springer Nature's AM terms of use, but is not the Version of Record and does not reflect post-acceptance improvements, or any corrections. The Version of Record is available online at: <http://dx.doi.org/10.1007/s12205-022-0567-6>

General rights

Unless a licence is specified above, all rights (including copyright and moral rights) in this document are retained by the authors and/or the copyright holders. The express permission of the copyright holder must be obtained for any use of this material other than for purposes permitted by law.

- Users may freely distribute the URL that is used to identify this publication.
- Users may download and/or print one copy of the publication from the University of Birmingham research portal for the purpose of private study or non-commercial research.
- User may use extracts from the document in line with the concept of 'fair dealing' under the Copyright, Designs and Patents Act 1988 (?)
- Users may not further distribute the material nor use it for the purposes of commercial gain.

Where a licence is displayed above, please note the terms and conditions of the licence govern your use of this document.

When citing, please reference the published version.

Take down policy

While the University of Birmingham exercises care and attention in making items available there are rare occasions when an item has been uploaded in error or has been deemed to be commercially or otherwise sensitive.

If you believe that this is the case for this document, please contact UBIRA@lists.bham.ac.uk providing details and we will remove access to the work immediately and investigate.

1 **Manuscript No. KSCE-D-22-00567**

2 **Relationship Between Dynamic Tensile Strength and Pore**
3 **Structure of Saturated Concrete under Lateral Pressure**

4 **Hao Wang ^{*1,3}, Licheng Wang², Bahman Ghiassi³, Yupu Song², Le Zhou¹, Dongxu Hou¹**

5 **1 School of Civil Engineering, Shenyang University, Shenyang 110044, China**

6 **2 State Key Laboratory of Coastal and Offshore Engineering, Dalian University of Technology,**

7 **Dalian 116024, China**

8 **3 Centre for Structural Engineering and Informatics, Faculty of Engineering, University of**

9 **Nottingham, Nottingham NG7 2RD, UK**

10
11
12
13
14
15
16
17
18
19
20

***Corresponding author. Tel: +86-188-42577100. E-mail: 830502wh@163.com.**

21 **Hao Wang, Senior lecturer, Mailing address : 21 Wanghua South Street, Dadong District,**
22 **Shenyang 110044, China**

23 **Licheng Wang, Professor; E-mail: wanglicheng2000@163.com**

24 **Bahman Ghiassi, Associate Professor; E-mail: Bahman.Ghiassi@nottingham.ac.uk**

25 **Yupu Song, Professor; E-mail: syupu@dlut.edu.cn**

26 **Le Zhou, Professor; E-mail: zhoule0306@126.com**

27 **Dongxu Hou, Associate Professor. E-mail: dongxv666@126.com**

ABSTRACT

The dynamic properties of concrete in two states (saturated and dry) were compared and analyzed through a series of dynamic biaxial tensile-compressive (T-C) experimentals. All specimens were subjected to constant biaxial T-C stress ratios (0.5:-1, 0.25:-1, 0.1:-1, 0.05:-1 and 1:0 respectively) at different strain rates (10^{-5}s^{-1} to 10^{-2}s^{-1}). It was found that the biaxial T-C ultimate strengths of both kinds concrete closely relate to the lateral pressure of the specimen, and the independent tensile and compressive strength increases with the increase of strain rate. In the case of exerting lateral pressure, the failure states of specimens show same manner as that of the uniaxial tensile specimens, which indicates that the specimens were completely fractured under tensile loading. The test results show that the biaxial T-C strength of saturated concrete is lower at strain rates of 10^{-5}s^{-1} , whereas it is higher at the other three strain rates (10^{-4}s^{-1} , 10^{-3}s^{-1} and 10^{-2}s^{-1}). This distinct difference indicates that saturated concrete is more rate sensitive under lateral pressure. Through mechanical analysis the article explains the reason of this phenomenon is mainly due to the beneficial tensile stress of the pore water surface and the Stefan effect. Meanwhile, the strength prediction expression of saturated concrete was established under the condition of stress ratio and strain rate are considered simultaneously.

Keywords: saturated concrete; experiment; tensile strength; biaxial T-C; lateral pressures; strain rates; strength prediction expression;

50 **1 Introduction**

51 There are lots of concrete structures that are often eroded by rain, and many hydraulic
52 structures and port engineering structures are in service in the water environment all
53 year round. The free water will penetrate into the concrete through numerous pores and
54 micro-cracks. These structures are not only often subjected to static loads, but also are
55 subjected to dynamic loads such as explosion, shock, and earthquake. Wang et al (2016),
56 Wu et al (2012) and Kaplan (1980) found that the properties of concrete have changed
57 significantly because of pore water in microcracks. Bischoff and Perry (1991), Fu et al
58 (1991), Malvarl and Ross (1998) thought the saturated concrete showed different
59 mechanical properties under different strain rate load conditions. The research on
60 saturated concrete is of great significance for the application of civil structural
61 engineering.

62 Some related research results show that the rate-sensitivity of concrete is closely
63 related to the free water in micro-cracks. Due to the internal defects of the concrete
64 itself, free water can penetrate into the micro-cracks of the concrete. Xuan et al (2009),
65 Liu et al (2011) and Zhang et al (2017) have shown that free water could reduce the
66 static strength of concrete. Rossi et al (1992) and Cadoni et al (2001) have found that the
67 dynamic strength of saturated concrete increased significantly. The study of Erzar and
68 Forquin (2011) indicated that when the strain rate was 20-150 s⁻¹, the strength of wet
69 concrete was 30% higher. Wang et al (2007, 2009) and Zhang et al (2015) found that
70 wet concrete was more sensitive to strain rate. Based on Rossi (1991), Zheng et al (2004,
71 2005) and Yan and Lin (2006) previous studies, it is speculated that the water is the

72 main factor for the increase of the dynamic strength of concrete. Bjerkei et al (1993) and
73 Morley (1979) showed that there was no difference in strength between saturated
74 concrete and dry concrete. Since the loading rate is too fast at the high strain rate of $1s^{-1}$,
75 the effect of water in the microcracks can be ignored due to the high local stress
76 intensity near the aggregates. However, some scholars had found that when hydraulic
77 concrete structures were in service, the concrete was under multi-axial loading state due
78 to water pressure, which should be considered in the design.

79 Ferrari and Granik (1995) considered that during the service of concrete structures,
80 concrete materials was often in a state of multiaxial complex stress, especially the
81 combination state of tensile-compressive loading is the most unfavorable to the concrete
82 structure. The tensile strength of concrete is significantly reduced in the presence of
83 lateral pressure, which will lead to susceptibility of concrete to cracking and thus steel
84 corrosion and reduction of service life. The concrete studied in this paper is a common
85 material for hydraulic structure and is submerged in water for a long time. Due to the
86 special service environment, the hydraulic concrete structure is under complex stress
87 state. At present, because of the lack of equipment and the difficulty of multi-axial load
88 test, only the experimental researches of uniaxial loading condition were carried out.
89 Although there have been some relevant studies on saturated concrete (Wang et al
90 (2016), Wu et al (2012), Xuan et al (2009), Liu et al (2011), Wang et al (2016), Zhao
91 and Wen (2018), Sun et al (2020) and Huang et al (2020)), these researches are limited
92 to uniaxial tensile, compressive, or impact loads. The evaluation of saturated concrete
93 under biaxial T-C stress state is very scarce. The influence of free water in micro-cracks

94 is not considered in the current design specifications. It is of great significance to study
 95 the properties of saturated concrete under the combined action of tensile and
 96 compressive loading. In this study, a large number of saturated concrete specimens were
 97 investigated by tensile tests under lateral pressure, and the prediction equation of biaxial
 98 T-C strength of saturated concrete was established.

99 **2. Materials and Experimental Program**

100 The concrete mixture ratio and specimen size used in this paper are shown in Table 1
 101 and Fig. 1, and the multi-axis test system used in this test and the installation of the
 102 specimens are shown in Fig. 2. Concrete specimen production and test details, please
 103 refer to Supplementary Material.

104 **Table 1 Mix Ratio of Specimen (unit: kg/m³).**

Sand	Cement	Fly ash	Water	Aggregate size (mm)			Water reducer
				3~20	21~40	41~80	
533	215	52	121	411.5	411.5	580	0.209

105

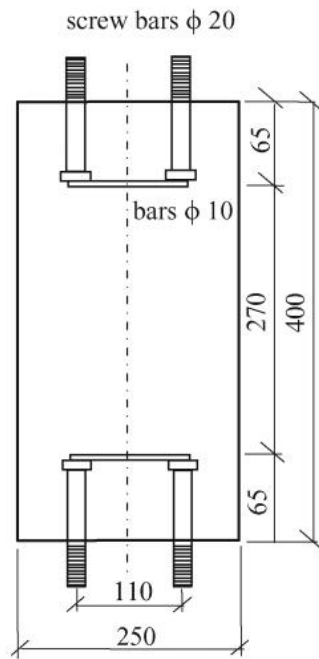
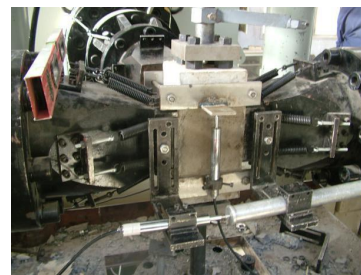


Fig. 1 Details of Specimen (unit: mm)



(a) Multi-axis Test Apparatus



(b) Installation of Specimen

Fig. 2 Test Instrument and Specimen Installation

3 The Results Discussed

3.1 Tensile Strength of Concrete under Lateral Pressure

The test results were listed in Table 2 and 3 respectively. The difference in strength between the two types of concrete is remarkable, in which it can be seen that all the strengths in both directions increase with increasing strain rate. We can clearly see from the results that the increase strength of saturated concrete was even higher. According to the current results, it may be the effect of pore water.

119 **Table 2 Dynamic Strengths of Saturated Concrete under Biaxial T-C Loading**

120 **(MPa)**

Stress ratio ($\sigma_1 : -\sigma_3$)	Strain rate							
	10^{-5}s^{-1}		10^{-4}s^{-1}		10^{-3}s^{-1}		10^{-2}s^{-1}	
1 : 0	1.63	0	2.22	0	2.55	0	2.91	0
0.05 : -1	0.42	8.4	0.76	15.2	0.91	18.2	1.19	23.8
0.1 : -1	0.59	5.9	0.98	9.8	1.21	12.1	1.63	16.3
0.25 : -1	0.97	3.88	1.48	5.92	1.77	7.08	2.03	8.12
0.5 : -1	1.24	2.48	1.73	3.46	2.07	4.14	2.43	4.86
0 : -1	0	-17.11	0	-26.16	0	-24.83	0	-27.82

121 **Table 3 Dynamic Strengths of Dry Concrete under Biaxial T-C Loading (MPa)**

Stress ratio ($\sigma_1 : -\sigma_3$)	Strain rate							
	10^{-5}s^{-1}		10^{-4}s^{-1}		10^{-3}s^{-1}		10^{-2}s^{-1}	
1 : 0	1.71	0	2.02	0	2.38	0	2.72	0
0.05 : -1	0.49	9.8	0.69	13.8	0.84	16.8	1	20
0.1 : -1	0.68	6.8	0.85	8.5	1.04	10.4	1.43	14.3
0.25 : -1	1.07	4.28	1.37	5.48	1.57	6.28	1.86	7.44
0.5 : -1	1.3	2.6	1.55	3.1	1.86	3.72	2.12	4.24
0 : -1	0	-20.34	0	-21.57	0	-23	0	-24.83

122 **3.2 Failure Mode**

123 From Fig. 3(a) and Fig. 3(b) we could see that, the failure patterns of concrete in the two

124 states are similar, and the failure patterns of concrete specimens have little relationship

125 with moisture content. The failures of both kind of specimens were very sudden and
126 showed a loud crack. Figure 4 shows that there is an obvious fracture crack in the
127 middle part of the concrete specimen, and the load direction of the specimen is
128 perpendicular to the fracture surface of the specimen, which indicates that the specimen
129 was completely fractured under tensile loading. The failure patterns of all concrete
130 specimens with all stress ratios are the same, indicating that the lateral pressure has little
131 affect on the damage modes of specimens. The failure of concrete specimens mainly
132 occurs in the transition zone of mortar at low loading rate. The existence of pore
133 water in micro-cracks of concrete weakens bonding force of mortar in transition zone.
134 Therefore, the static properties of saturated concrete depend more on the effects of pore
135 water between mortar and transitional zone. The number of aggregates fracture
136 increases with the increasing strain rate.

137 Under dynamic biaxial T-C loading, both kinds of concrete specimens are
138 accompanied by some fragments at the fracture section. A large number of micro-cracks
139 form the fracture area, and finally fragments appear. The size of the macroscopic crack
140 is determined by the lateral pressure, and the extension and development effect of micro
141 crack is not obvious when the lateral pressure is less. On the contrary, there are several
142 macroscopic cracks in the fracture surface of the concrete specimen.



143

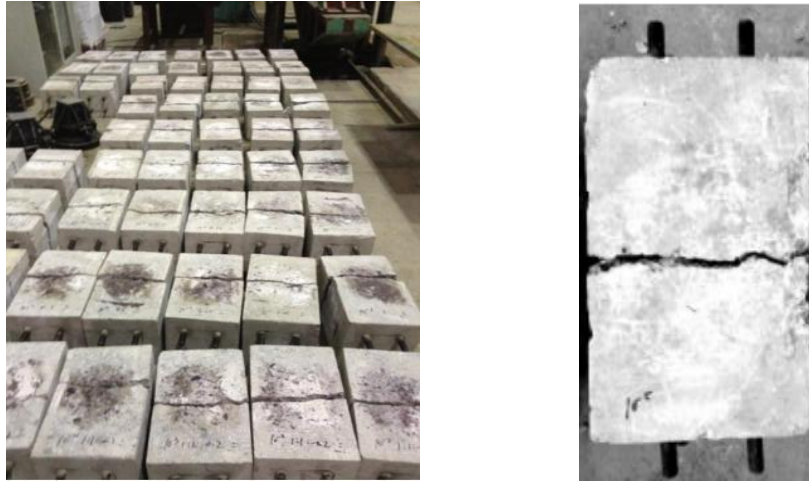
144

(a) Saturated

(b) Dry

145

Fig. 3 Failure Surfaces of Specimens



146

147

(a) Biaxial T-C

(b) Tensile Load

148

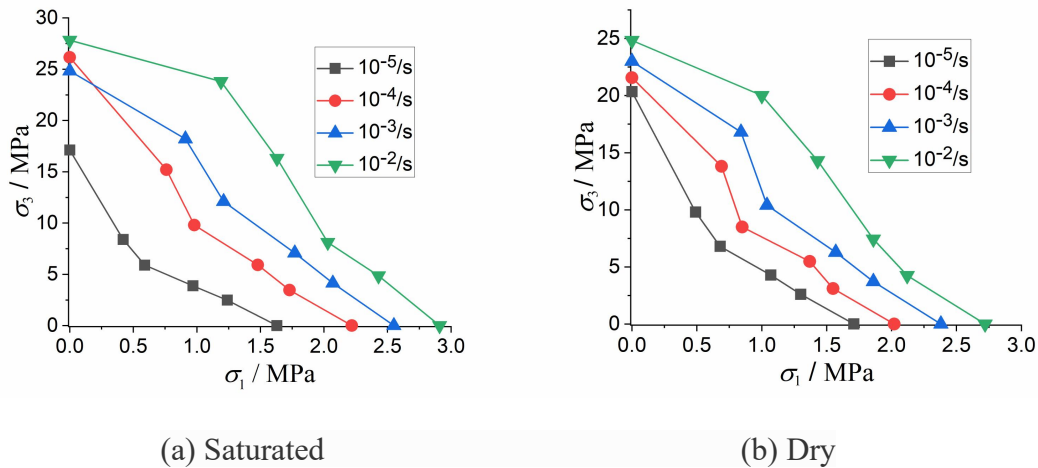
Fig. 4 Image of Specimen Failure

149 3.3 Effect of Strain Rate

150 From Table 2 and 3 we can see that the uniaxial strength is much higher than that of the
151 biaxial T-C strength at all strain rate conditions. The lateral pressure strength (σ_3) and
152 tensile strength (σ_1) of concrete in both directions increase with the increasing strain rate.
153 The $10^{-5}s^{-1}$ was defined as static condition in this study, and at the static loading
154 condition, both σ_1 and σ_3 of saturated concrete are lower at the same stress ratio. In
155 contrast, the strength (σ_1, σ_3) of saturated concrete are higher. This may be caused by
156 free water in the micro-cracks of saturated concrete specimen. Under the static loading
157 conditions, the water pressure in the micro-crack promotes the crack expansion and
158 reduces the strength of concrete. But due to the high loading rate and the viscous effect
159 of water, the reverse tensile stress that inhibits the crack propagation is generated
160 instantly, which lead to the strength increase.

161 3.4 The Influence of the Presence of Lateral Pressure

162 It is obvious that the uniaxial strength is much higher than that of the biaxial T-C
 163 strength at any strain rate condition. It could be found that the tensile strength decreases
 164 with the increase of lateral pressure from Fig. 5 for comparison. It is found that the
 165 failure strength are strongly influenced by the magnitude of lateral pressure from the
 166 test results. The variation law of lateral pressure and strain rate in Fig.5. The lateral
 167 pressure strength (σ_3) decreasing with the absolute value of stress ratios increasing, the
 168 strength of the combined loading (tensile loading and lateral pressure) is much lower
 169 than the uniaxial lateral pressure strength. It indicates that due to the greater lateral
 170 pressure, the concrete is more likely to be damaged under tensile load.



171
172 (a) Saturated (b) Dry
173 **Fig. 5 Variation Law of Tensile Strength with Lateral Pressure**

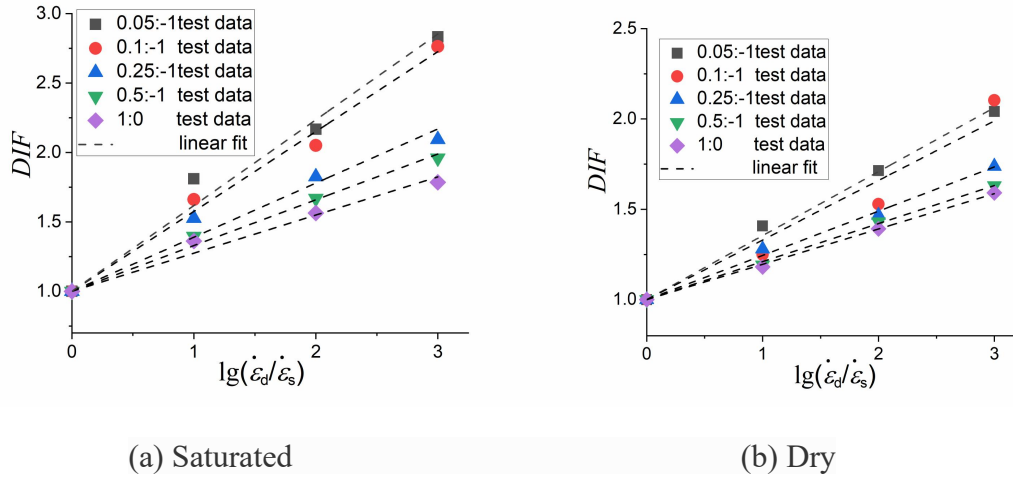
174 **3.5 Dynamic Increase Factor (DIF)**

175 In Fig. 6, the tensile strength changes with the increasing strain rate at different lateral
 176 pressure. However, the strength of concrete increases by different degrees at different
 177 stress combinations. Through fitting analysis of test data, the following formula can
 178 well describe the growth range of dynamic strength of concrete .

$$DIF = \frac{\sigma_t^d}{\sigma_t^s} = 1 + a \lg \left(\frac{\dot{\varepsilon}_d}{\dot{\varepsilon}_s} \right) \quad (1)$$

179

180 where $\dot{\varepsilon}_s$ is defined as 10^{-5}s^{-1} ; $\dot{\varepsilon}_d$ is the current strain rate (In this paper, they are
 181 10^{-5}s^{-1} , 10^{-4}s^{-1} , 10^{-3}s^{-1} and 10^{-2}s^{-1} , respectively); σ_t^s and σ_t^d are static and dynamic tensile
 182 strengths respectively, and correlation coefficients a are shown in Table 4.



183

184

185

Fig. 6 DIF Versus Strain Rate for Saturated and Dry Concrete

186

Table 4 Test Regression Parameters and the Correlation Coefficient

Types of concrete	Fitting parameter	Stress ratio ($\sigma_1 : -\sigma_3$)				
		1:0	0.05:-1	0.1:-1	0.25:-1	0.5:-1
Saturated	a	0.256	0.586	0.568	0.358	0.315
concrete	R^2	0.9704	0.9707	0.9832	0.9577	0.9891
Dry	a	0.339	0.168	0.244	0.257	0.277
concrete	R^2	0.9988	0.9939	0.9339	0.9917	0.9975

187

3.6 Influence of Pore Water in Microcracks on Tensile Strength of Concrete

188

It's obvious that the failure patterns of concrete specimen are typical tensile failure, and

189

the damage is mainly induced by the action of tensile loading, while implies that the

190 lateral pressure accelerates the tensile failure of the specimen, and the ultimate tensile
191 strength decreases obviously with the increase in lateral pressure. It is also found that
192 the sensitivity of saturated concrete to strain rate may be caused by the viscous effect of
193 water.

194 The spread of micro-cracks leads to the failure of concrete, so the free water in
195 pores will play a significant role in the change of concrete strength. According to the
196 Griffith Microcrack Theory, the fracture is not caused by the pulling of two parts of the
197 body along the interface, but by the internal micro-cracks growth. The stress that makes
198 the crack start to grow is regarded as the ultimate tensile strength of concrete is
199 proposed by Bazant and Planas (1998).

$$\sigma = \sqrt{\frac{2E\gamma}{\pi c}} \quad (2)$$

200
201 where σ is the stress that causes the crack to spread, γ is the concrete surface energy of
202 microcrack propagation, c is the semi-length of microcrack inside concrete, and E is
203 elastic modulus of concrete. According to the microcrack theory, the surface energy of
204 concrete material is the main factor which influences the ultimate tensile strength.
205 Based on the surface physicochemical theory of Prutton (1983), the film pressure of
206 solid surface immersed in water is lower than that is not immersed in water. In this case,
207 the surface tension of saturated concrete is much lower. The specific formula is as
208 follows,

$$\gamma' = \gamma - \gamma_0 \quad (3)$$

209
210 where γ' stands for the surface energy of saturated concrete, γ is the surface energy of
211 dry concrete, γ_0 is the reduced surface energy.

212 Under the condition of dynamic loading, the micro-cracks in the concrete extend
213 and expand rapidly, resulting in fracture and failure of the concrete specimen. The free
214 water doesn't have enough time to reach the crack tip due to the rapid crack propagation,
215 the direction of free water surface tension is opposite to the direction of crack
216 propagation, which inhibits the crack development in a short time. The dynamic biaxial
217 T-C strength of concrete is improved, and the free water surface tension which prevents
218 crack propagation is expressed by Prutton (1983),

$$\sigma_c = \frac{2\gamma \cos \theta}{\rho} \quad (4)$$

219 where γ stands for the free water surface energy, θ is the wetting angle, and ρ is radius of
220 curvature of liquid.
221

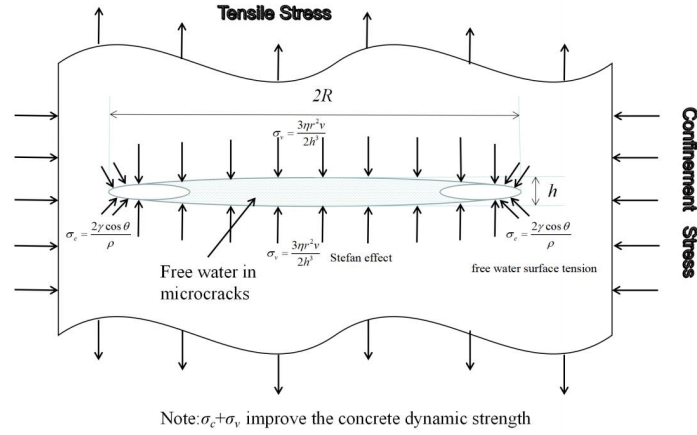
222 From the physical point of view according to Stefan effect, the improvement of
223 concrete dynamic strength compared with quasi-static strength is given by Zheng and Li
224 (2004) and Rossi (1991),

$$\sigma_v = \frac{3\eta r^2 v}{2h^3} \quad (5)$$

225 where η is the water viscosity coefficient, h is the width of the crack, and r is radius
226 of plates. From the above formula, when concrete is subjected to dynamic load, the
227 loading rate v increases and the cohesive force also increases, which prevents the
228 expansion of cracks. Within a certain loading rate range, reverse cohesion that prevents
229 crack propagation can be obtained by Eq. (5). The free water surface tension and the
230 free water viscous stress is considered simultaneously, the following formula is
231 obtained,
232

233
$$\sigma = \frac{2\gamma \cos \theta}{\rho} + \sigma_v \quad (6)$$

234 Under the condition of dynamic lateral pressure, the increasing mechanism of
 235 dynamic tensile strength can be explained by the following schematic diagram Fig. 7.



236
 237 **Fig.7. Schematic Diagram of Tensile Strength Increase of Saturated Concrete**

238 Based on the concept of wet weakening, Pihlajavaara(1974) found the following
 239 relation equation:

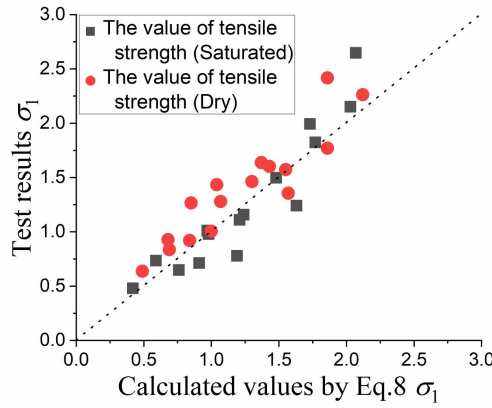
240
$$\frac{f_t^{sat}}{f_t^{dry}} = \sqrt{1 - cS_r} \quad (7)$$

241 where f_t^{sat} is the splitting tensile strength at saturation; f_t^{dry} is the splitting tensile strength
 242 at dry state; c is the correlation coefficient; and S_r is saturation ratio.

243 On the basis of considering saturation and strain rate factor, we establish the
 244 expression of biaxial T-C strength of concrete in principal stress space.

245
$$\frac{\sigma_1}{f_t} = \left[\frac{A\alpha}{1 + A\alpha} + B(1 - e^{-C\alpha}) \cdot \lg(\dot{\epsilon}_d / \dot{\epsilon}_s) \right] \cdot (1 - DS_r)^{1/2} \quad (8)$$

246 where f_t is uniaxial tensile strength; σ_1 is dynamic biaxial T-C strength of concrete; α is
 247 stress ratio, S_r is saturation ratio, and A, B, C, D are the correlation coefficient.



248

249

Fig. 8. Comparison of Test Results and Calculated Values

250

The factors of saturation, strain rate and lateral pressure was considered in the

251

tensile strength criterion in this paper. It could be clearly seen that the calculated results

252

were close to the test results in Fig. 8. However, due to the discrete nature of concrete,

253

very few scattered data results could be ignored. The relative error range between the

254

prediction results and the test results are from 1.3% to 20%. Therefore, the proposed

255

strength relationship was considered reasonable.

256

4. Strength Criteria in Octahedral Space

257

Through the analysis of the test results of both kinds concrete under different strain rates,

258

the triaxial principal stress is transformed into octahedral stress. The octahedral normal

259

stress (σ_{oct}) and octahedral shear stress (τ_{oct}) are calculated by the following formula. In

260

octahedral space, similarity θ represents the direction of shear stress (τ_{oct}).

261

$$\sigma_{oct} = \frac{1}{3}(\sigma_1 + \sigma_2 + \sigma_3) \quad (9)$$

262

$$\tau_{oct} = \frac{1}{3} \left[(\sigma_1 - \sigma_2)^2 + (\sigma_1 - \sigma_3)^2 + (\sigma_2 - \sigma_3)^2 \right]^{1/2} \quad (10)$$

263

$$\theta = \arccos \frac{2\sigma_1 - \sigma_2 - \sigma_3}{3\sqrt{2}\tau_{oct}} \quad (11)$$

264

The σ_{oct}/f_c and τ_{oct}/f_c are listed in Table 5 and 6.

265

Table 5 Octahedron Space Biaxial T-C Stress of Saturated Concrete

Stress ratio ($\sigma_1 : -\sigma_3$)	Strain rate							
	10^{-5}s^{-1}		10^{-4}s^{-1}		10^{-3}s^{-1}		10^{-2}s^{-1}	
0.05:-1	-0.16	0.24	-0.28	0.43	-0.34	0.51	-0.44	0.67
0.1:-1	-0.1	0.17	-0.17	0.28	-0.21	0.35	-0.29	0.47
0.25:-1	-0.06	0.12	-0.09	0.19	-0.1	0.22	-0.12	0.26
0.5:-1	-0.02	0.09	-0.03	0.13	-0.04	0.15	-0.05	0.18

266

267

Table 6 Octahedron Space Biaxial T-C Stress of Dry Concrete

Stress ratio ($\sigma_1 : -\sigma_3$)	Strain rate							
	10^{-5}s^{-1}		10^{-4}s^{-1}		10^{-3}s^{-1}		10^{-2}s^{-1}	
0.05:-1	-0.16	0.25	-0.23	0.35	-0.28	0.42	-0.33	0.5
0.1:-1	-0.11	0.18	-0.13	0.22	-0.16	0.27	-0.22	0.37
0.25:-1	-0.06	0.12	-0.07	0.15	-0.08	0.18	-0.1	0.21
0.5:-1	-0.02	0.08	-0.03	0.1	-0.03	0.12	-0.04	0.14

268

269 By analyzing the dynamic strength of both concrete, the failure criterion of

270 octahedral space are established:

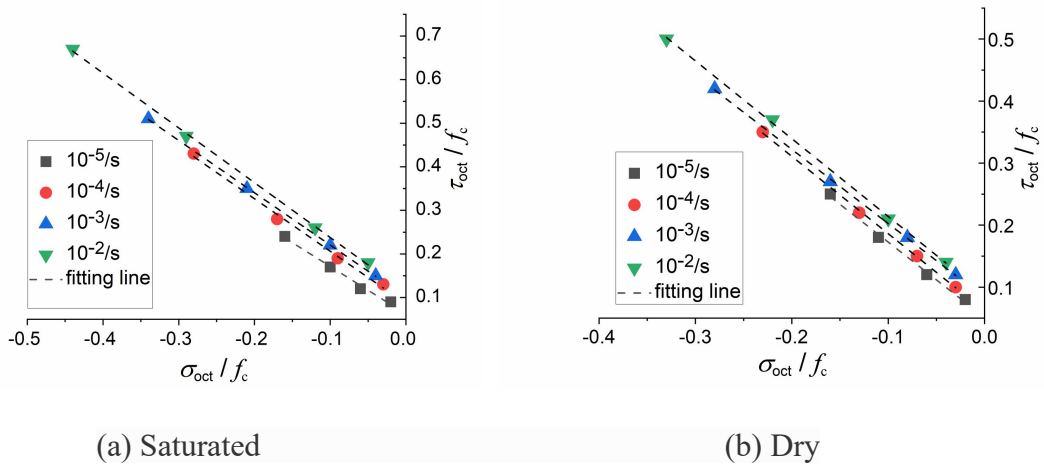
$$271 \quad \frac{\tau_{oct}^d}{f_c} = a + b \frac{\sigma_{oct}^d}{f_c} + c \lg(\dot{\varepsilon}_d / \dot{\varepsilon}_s) \quad (12)$$

272 where f_c stands for static uniaxial compressive strength, $\dot{\varepsilon}_s$ and $\dot{\varepsilon}_d$ are the same values

273 represented by Eq.(1) in this paper. ($\dot{\varepsilon}_d = \dot{\varepsilon}_s$, σ_{oct}^d , τ_{oct}^d represents the static octahedral

274 normal stress and shear stresses respectively, $\dot{\varepsilon}_d > \dot{\varepsilon}_s$, σ_{oct}^d , τ_{oct}^d represents dynamic
 275 variable field). a , b and c are the regression parameters. For saturated concrete: $a =$
 276 0.055 , $b = -1.224$, $c = 0.022$, $R^2 = 0.997$. For dry concrete: $a = 0.049$, $b = -1.232$, $c =$
 277 0.014 , $R^2 = 0.999$.

278 As can be seen from the value of R^2 , it could be determined the Eq.(12) can be
 279 suitable for dynamic T-C failure criterion in octahedral space. Fig. 9 shows the fitting
 280 line of the biaxial T-C in octahedral space which is very close to the experimental
 281 results. It illustrates that Eq. (12) is more reasonable to express the failure criterion in
 282 octahedral space for two kinds of concrete.



283
 284 (a) Saturated (b) Dry
 285 **Fig. 9 Biaxial T-C Failure Criterion in Octahedral Space of Concrete under**
 286 **Various Strain Rates**

287 5. Conclusions

288 In this paper, the servo hydraulic multiaxial test system is used to carry out dynamic
 289 tensile test on saturated and dry concrete with five different variations of lateral pressure.

290 The conclusions are obtained through the test of 120 concrete specimens.

291 (1) The uniaxial tensile strength of concrete is much higher than ultimate biaxial T-C

292 strength in the presence of lateral pressure in all strain rate ranges. Lateral pressure
293 plays an decisive role in ultimate tensile strength.

294 (2) The factors of lateral pressure and strain rate are considered simultaneously, the
295 failure criterion in octahedral space was proposed which are very suitable to express the
296 biaxial T-C strength of both concrete.

297 (3) Although the failure modes of both concrete are the same as those of uniaxial tensile
298 dynamic specimens, the ultimate biaxial T-C strength is lower, and concrete structures
299 are more prone to failure under multi-axial complex stress states, especially under the
300 combination of tensile and compressive loading. And the failure patterns of concrete
301 specimens have little relationship with moisture content.

302 (4) In the current research, the dynamic strength of saturated concrete increases is even
303 more dramatic. This indicates that the tensile strength of saturated concrete is more
304 easily affected by strain rate in the presence of lateral pressure. The beneficial tensile
305 stress of the free water surface and the Stefan effect are the main factors for inducing
306 the enhancement of strength. In this study, the strength prediction expression (Eq.(8)) of
307 saturated concrete was established which the stress ratio and strain rate are considered
308 simultaneously, and the prediction expression is more reasonable by comparing with the
309 test results.

310

311 **Acknowledgments**

312 This study is supported by the National Natural Science Foundation of China (grant No.
313 51079019; 51378090; 51978416) and China Scholarship Council (No. (2019) 75) and

314 Young and Middle-aged Innovative Talents Support Program of Shenyang Science and
315 Technology Bureau (No. RC190199).

316

317 **References**

318 Bjerkei L, Jensen JJ, Lenschow R (1993) Strain development and static compressive
319 strength of concrete exposed to water pressure loading. *ACI Structural Journal* 90
320 (3): 310–315.

321 Bischoff PH, Perry SH (1991) Compressive behaviour of concrete at high strain rates.
322 *Materials and Structures* 24 (6): 425–450, [DOI:10.1007/BF02472016](https://doi.org/10.1007/BF02472016)

323 Bazant ZP, Planas J (1998) *Fracture and Size Effect in Concrete and Other Quasibrittle*
324 *Materials*, CRC Press, Boca Raton, USA.

325 Cadoni E, Labibes K, Albertini C (2001) Strain-rate effect on the tensile behaviour of
326 concrete at different relative humidity levels, *Materials and Structures* 34: 21–26,
327 [DOI:10.1007/BF02472446](https://doi.org/10.1007/BF02472446)

328 Erzar B, Forquin P (2011) Free water influence on the dynamic tensile behaviour of
329 concrete. *Applied Mechanics & Materials* 82:45–50,
330 [DOI:10.4028/www.scientific.net/AMM.82.45](https://doi.org/10.4028/www.scientific.net/AMM.82.45)

331 Fu HC, Erki MA, Seckin M (1991) Review of effects of loading rate on concrete in
332 compression. *Journal of Structural Engineering* 117(12):3645–3659.
333 [DOI:10.1061/\(ASCE\)0733-9445\(1991\)117:12\(3645\)](https://doi.org/10.1061/(ASCE)0733-9445(1991)117:12(3645))

334 Ferrari M, Granik VT. (1995) Ultimate criteria for materials with different properties in
335 biaxial tension and compression: a micromechanical approach. *Materials Science*

336 and Engineering: A 202(1–2):84–93. DOI:10.1016/0921-5093(95)09788-0

337 Huang XP, Kong XZ, Hu J , Zhang XD, Zhang ZT, Fang Q (2020) The influence of free
338 water content on ballistic performances of concrete targets. International Journal of
339 Impact Engineering 139:103530, DOI:10.1016/j.ijimpeng.2020.103530

340 He ZJ, Song YP (2010) Triaxial strength and failure criterion of plain high-strength and
341 high-performance concrete before and after high temperatures. Cement Concrete
342 Research 40: 17-18, DOI:10.1016/j.cemconres.2009.08.024

343 Kaplan SA (1980) Factors affecting the relationship between rate of loading and
344 measured compressive strength of concrete. Magazine of Concrete Research
345 32:79–88, DOI:10.1680/macr.1980.32.111.79

346 Liu B , Li P, Li L (2011) Experimental study on influence of water content on concrete
347 strength. Journal of Beijing Jiaotong University 35: 9–12 (in Chinese), DOI :
348 10.1631/jzus.A1000209

349 Morley CT (1979) Theory of pore pressure in concrete cylinders. ACI Materials Journal
350 76 (3–4): 7–45.

351 Mauro F, Grinik VT (1995) Ultimate criteria for materials with different properties in
352 biaxial tension and compression: a micromechanical approach. Materials Science
353 and engineering :A 202(1–2): 84–93, DOI:10.1016/0921-5093(95)09788-0

354 MalvarL J , Rossc A (1998) Review of strain rate effects for concrete in tension. ACI
355 Materials Journal 95: 435–439.

356 Prutton M (1983) Surface Physics, Clarendon Press, Oxford, UK.

357 Pihlajavaara SE (1974) A review of some of the main results of a research on the aging

358 phenomena of concrete: effect of moisture conditions on strength, shrinkage and
359 creep of mature concrete. *Cement and Concrete Research* 4:761–771.

360 Rossi P (1991) A physical phenomenon which can explain the mechanical behavior of
361 concrete under high strain rates. *Materials and Structures* 24:422-424,
362 [DOI:10.1007/BF02472015](https://doi.org/10.1007/BF02472015)

363 Rossi P (1991) Influence of cracking in the presence of free water on the mechanical
364 behaviour of concrete. *Magazine of Concrete Research* 43: 53–57,
365 [DOI:10.1680/mac.1991.43.154.53](https://doi.org/10.1680/mac.1991.43.154.53)

366 Rossi P, VanMier JGM, Boulay C (1992) The dynamic behaviour of concrete: influence
367 of free water. *Materials and Structures* 25: 509–514, [DOI:10.1007/BF02472446](https://doi.org/10.1007/BF02472446)

368 Shang HS (2013) Triaxial T–C behavior of air-entrained concrete after freeze–thaw
369 cycles. *Cold Regions Science Technology* 89:1-6,
370 [DOI:10.1016/j.coldregions.2013.01.004](https://doi.org/10.1016/j.coldregions.2013.01.004)

371 Shang HS, Song YP (2006) Experimental study of strength and deformation of plain
372 concrete under biaxial compression after freezing and thawing cycles. *Cement*
373 *Concrete Research* 36: 1857–64, [DOI:10.1016/j.cemconres.2006.05.018](https://doi.org/10.1016/j.cemconres.2006.05.018)

374 Shang HS, Song YP(2010) Performance of plain concrete under biaxial
375 tension–compression after freeze–thaw cycles. *Magazine of Concrete Research* 62:
376 149–55, [DOI:10.1680/mac.2008.62.2.149](https://doi.org/10.1680/mac.2008.62.2.149)

377 Sun XY, Wang HL, Cheng XD, Sheng YF (2020) Effect of pore liquid viscosity on the
378 dynamic compressive properties of concrete. *Construction and Building Materials*
379 231: 117143, [DOI:10.1016/j.conbuildmat.2019.117143](https://doi.org/10.1016/j.conbuildmat.2019.117143)

380 Shi LL, Wang LC, Song YP, Shen L (2014) Dynamic multiaxial strength and failure
381 criterion of dam concrete. *Construction and Building Materials* 66:181-191,
382 [DOI:10.1016/j.conbuildmat.2014.05.076](https://doi.org/10.1016/j.conbuildmat.2014.05.076)

383 Shen L, Wang LC, Song YP, Shi LL (2017) Comparison between dynamic mechanical
384 properties of dam and sieved concrete under biaxial tension-compression.
385 *Construction and Building Materials* 132:43-50,
386 [DOI:10.1016/j.conbuildmat.2016.11.113](https://doi.org/10.1016/j.conbuildmat.2016.11.113)

387 Wu SX, Chen XD, Zhou JK (2012) Influence of strain rate and water content on
388 mechanical behavior of dam concrete. *Construction and Building Materials* 36:
389 448–457, [DOI:10.1016/j.conbuildmat.2012.06.046](https://doi.org/10.1016/j.conbuildmat.2012.06.046)

390 Wang HL, Jin WL, Li QB (2009) Saturation effect on dynamic tensile and compressive
391 strength of concrete. *Advanced Structural Engineering* 12:279–286,
392 [DOI:10.1260/136943309788251713](https://doi.org/10.1260/136943309788251713)

393 Wang HL, Li QB (2007) Experiments of the compressive properties of dry and saturated
394 concrete under different loading rates. *Journal of Hydraulic Engineering* 26:84–89
395 (in Chinese), [DOI: 10.1007/s10870-007-9222-9](https://doi.org/10.1007/s10870-007-9222-9)

396 Wang QF, Liu YH, Peng G (2016) Effect of water pressure on mechanical behavior of
397 concrete under dynamic compression state. *Construction and Building Materials* 125:
398 501-509, [DOI:10.1016/j.conbuildmat.2016.08.058](https://doi.org/10.1016/j.conbuildmat.2016.08.058)

399 Wang HL, Song YP (2009) Behavior of dam concrete under biaxial
400 compression–tension and triaxial compression–compression–tension. *Materials and*
401 *Structures* 42: 241–9, [DOI:10.1617/s11527-008-9381-y](https://doi.org/10.1617/s11527-008-9381-y)

402 Wang H, Wang LC, Song YP (2016) Influence of free water on dynamic behavior of
403 dam concrete under biaxial compression. Construction and Building Materials
404 112:222–231, [DOI:10.1016/j.conbuildmat.2016.02.090](https://doi.org/10.1016/j.conbuildmat.2016.02.090)

405 Xuan HV , Malecot Y, Daudeville L (2009) Experimental analysis of concrete behavior
406 under high confinement: effect of the saturation ratio. International Journal of Solid
407 Structures 46:1105–1120, [DOI:10.1016/j.ijsolstr.2008.10.015](https://doi.org/10.1016/j.ijsolstr.2008.10.015)

408 Yan DY, Lin G (2006) Dynamic properties of concrete in direct tension. Cement
409 Concrete Research 36: 1371–1378, [DOI:10.1016/j.cemconres.2006.03.003](https://doi.org/10.1016/j.cemconres.2006.03.003)

410 ZdenekP B, Jaime P (1998) Fracture and Size Effect in Concrete and Other Quasibrittle
411 Materials, CRC Press, Boca Raton, USA.

412 Zheng D, Li QB (2004) An explanation for rate effect of concrete strength based on
413 fracture toughness including free water viscosity. Engineering Fracture Mechanics
414 71: 2319–2327, [DOI:10.1016/j.engfracmech.2004.01.012](https://doi.org/10.1016/j.engfracmech.2004.01.012)

415 Zheng D, Li QB, Wang L (2005) A microscopic approach to rate effect on compressive
416 strength of concrete. Engineering Fracture Mechanics 72: 2316–2327.
417 [DOI:10.1016/j.engfracmech.2005.01.012](https://doi.org/10.1016/j.engfracmech.2005.01.012)

418 Zhang GH, Li ZL, Zhang LF(2017) Experimental research on drying control condition
419 with minimal effect on concrete strength. Construction and Building Materials 135:
420 194–202, [DOI:10.1016/j.conbuildmat.2016.12.141](https://doi.org/10.1016/j.conbuildmat.2016.12.141)

421 Zhao FQ, Wen HM (2018) Effect of free water content on the penetration of concrete,
422 International Journal of Impact Engineering 121:180-190,
423 [DOI:10.1016/j.ijimpeng.2018.06.007](https://doi.org/10.1016/j.ijimpeng.2018.06.007)

424 Zhang Y, Zhu D, Li Y (2015) Dynamic mechanical properties of dry and saturated
425 concretes and their mechanism. *Explosion Shock Waves* 35:864–870 (in Chinese),
426 [DOI:10.11883/1001-1455\(2015\)06-0864-07](https://doi.org/10.11883/1001-1455(2015)06-0864-07)